Biochimica et Biophysica Acta 1837 (2014) 73–84

Contents lists available at ScienceDirect

Biochimica et Biophysica Acta

journal homepage: www.elsevier.com/locate/bbabio

The branched mitochondrial respiratory chain from *Debaryomyces hansenii*: Components and supramolecular organization

Alfredo Cabrera-Orefice, Natalia Chiquete-Félix, Juan Espinasa-Jaramillo, Mónica Rosas-Lemus, Sergio Guerrero-Castillo, Antonio Peña, Salvador Uribe-Carvajal *

Dept. of Molecular Genetics, Instituto de Fisiología Celular, Universidad Nacional Autónoma de México, Mexico City, Mexico

ARTICLE INFO

Article history:
Received 12 June 2013
Received in revised form 23 July 2013
Accepted 25 July 2013
Available online 7 August 2013

Keywords:
Respiratory chain
Debaryomyces hansenii
Alternative oxidase
Alternative NADH dehydrogenase
Glycerol-phosphate dehydrogenase
Supercomplexes

ABSTRACT

The branched respiratory chain in mitochondria from the halotolerant yeast *Debaryomyces hansenii* contains the classical complexes I, II, III and IV plus a cyanide-insensitive, AMP-activated, alternative-oxidase (AOX). Two additional alternative oxidoreductases were found in this organism: an alternative NADH dehydrogenase (NDH2e) and a mitochondrial isoform of glycerol-phosphate dehydrogenase ($_{Mit}$GPDH). These monomeric enzymes lack proton pump activity. They are located on the outer face of the inner mitochondrial membrane. NDH2e oxidizes exogenous NADH in a rotenone-insensitive, flavone-sensitive, process. AOX seems to be constitutive; nonetheless, most electrons are transferred to the cytochromic pathway. Respiratory supercomplexes containing complexes I, III and IV in different stoichiometries were detected. Dimeric complex V was also detected. In-gel activity of NADH dehydrogenase, mass spectrometry, and cytochrome *c* oxidase and ATPase activities led to determine the composition of the putative supercomplexes. Molecular weights were estimated by comparison with those from the yeast *Y. lipolytica* and they were IV_2, I–IV, III_2–IV_4, V_2, I–III_2, I–III_2–IV, I–III_2–IV_2, I–III_2–IV_3 and I–III_2–IV_4. Binding of the alternative enzymes to supercomplexes was not detected. This is the first report on the structure and organization of the mitochondrial respiratory chain from *D. hansenii*.

1. Introduction

The halotolerant, non-pathogenic, oleaginous yeast *Debaryomyces hansenii* is found in the sea and other hyperosmotic habitats [1,2]. *D. hansenii* grows in various environmental conditions including different salt concentrations [3–5], low temperatures [3] and different pHs [3,6]. In addition, *D. hansenii* assimilates many different carbon sources [7–9]. The ability of this yeast to synthesize and store lipids is used in biotechnology to make products of commercial interest, such as cheese [2,10].

D. hansenii has high aerobic metabolism and low fermentative activity which are enhanced by high extracellular NaCl or KCl [11–13]. Isolated *D. hansenii* mitochondria undergo permeability transition due to the opening of a mitochondrial unspecific channel (MUC) [14]. Both, the MUCs from *D. hansenii* ($_{Dh}$MUC) and *S. cerevisiae* ($_{Sc}$MUC) are regulated by effectors such as phosphate, Mg^{2+} or Ca^{2+} [14–19]. The $_{Dh}$MUC is the only MUC reported to date that is closed by Na^+ or K^+ [14] probably accounting for the monovalent cation coupling effects observed in whole yeast [12,13].

The mammalian oxidative phosphorylation system contains the four "orthodox" respiratory complexes (I, II, III and IV) plus the F_1F_O-ATP synthase (complex V) [20]. In addition to the above, mitochondria from plants, fungi, protozoa and some animals may contain "alternative" redox enzymes that substitute or coexist with the classical complexes; e.g. alternative NADH dehydrogenases and oxidases [21–25]. In fungi a mammalian-like respiratory complex may be substituted by an alternative enzyme, e.g. in *S. cerevisiae* complex I the oxidoreductase activity was substituted by an internal alternative NADH dehydrogenase [26,27].

The fungal alternative oxidases (AOXs) are single subunit proteins bound to the matrix side of the inner mitochondrial membrane (IMM) [28–31]. The cyanide-resistant AOX transfers electrons from ubiquinol to oxygen. AOX is inhibited by hydroxamic acids and by *n*-alkyl-gallates [29,32]. The presence of AOX constitutes an uncoupled branch of the respiratory chain probably designed to prevent substrate overload and overproduction of reactive oxygen species (ROS) [25,28,33–36].

Alternative type II NADH dehydrogenases (NDH2s) transfer electrons from NADH to ubiquinone without pumping protons [37]. NDH2s are monomeric proteins bound to the inner (NDH2i) or the outer (NDH2e) face of IMM [21,37]. NDH2s are not sensitive to rotenone, but instead are specifically inhibited by flavone [38].

Abbreviations: ADP, adenosine diphosphate; AMP, adenosine monophosphate; AOX, alternative oxidase; BN, blue-native; COX, cytochrome *c* oxidase; CRR, cyanide-resistant respiration; Dig, digitonin; IMM, inner mitochondrial membrane; LC-MS, liquid chromatography mass spectrometry; LM, laurylmaltoside; $_{Mit}$GPDH, glycerol-phosphate dehydrogenase (mitochondrial isoform); MUC, mitochondrial unspecific channel; MW, molecular weight; NDH, NADH dehydrogenase activity; NDH2e, alternative external NADH dehydrogenase; PAGE, polyacrylamide-gel electrophoresis; PG, propyl-gallate; ROS, reactive oxygen species; SDS, sodium dodecyl sulfate; 2D, second dimension

* Corresponding author at: Departamento de Genética Molecular, Instituto de Fisiología Celular, Universidad Nacional Autónoma de México, Ciudad Universitaria, Apdo. Postal 70–242, Mexico City, Mexico. Tel.: +52 55 5622 5632; fax: +52 55 5622 5630.
E-mail address: suribe@ifc.unam.mx (S. Uribe-Carvajal).

0005-2728/$ – see front matter © 2013 Elsevier B.V. All rights reserved.
http://dx.doi.org/10.1016/j.bbabio.2013.07.011

The mitochondrial isoform of glycerol-phosphate dehydrogenase ($_{Mit}$GPDH) is another component of branched respiratory chains [39,40]. $_{Mit}$GPDH oxidizes glycerol-phosphate to dihydroxyacetone-phosphate and reduces ubiquinone. Also, this protein is located on the outer face of the IMM [41]. The peripheral proteins NDH2s, $_{Mit}$GPDH and AOX are not proton pumps [21,29,40].

Two major models describe the structure/function relationship of the respiratory chain. The *fluid* or *random collision* model proposes that respiratory complexes float freely within the IMM and electron transport occurs through the diffusible carriers ubiquinone and cytochrome *c* [42]. On the other hand, the *solid* model proposes that respiratory complexes are organized into stable hetero-oligomers (supercomplexes or "respirasomes") that channel electrons between them [43–46]. There are data that support each model [47]. Kinetic studies show that each respiratory complex can be purified individually, retaining activity [42]. By contrast, blue native gel polyacrylamide electrophoresis (BN-PAGE) reveals the existence of supercomplexes composed of several respiratory complexes [48]. Respiratory supercomplexes can be observed when solubilizing mitochondrial membranes with small amounts of mild detergents such as digitonin [44]. The presence of respiratory supercomplexes has been well documented in mammals [48,49], plants [43,46,50] and different yeast species [51–54]. Additionally, a third model has been proposed: the *plasticity* model, where respiratory complexes undergo a dynamic association-dissociation process and isolated supercomplexes transfer electrons from NADH to oxygen [55]. The plasticity model suggests that complex association/dissociation regulates oxidative phosphorylation [55,56].

Here, the mitochondrial respiratory chain of *D. hansenii*, which has been reported to contain all four mammalian-like respiratory complexes [57] plus a putative stationary-phase-inducible AOX, was characterized [58,59]. This branched respiratory chain contains all the complexes reported [59] plus an external NDH2 and a glycerol-phosphate dehydrogenase. In addition, association of these complexes in different supercomplexes was observed.

2. Materials and methods

2.1. Chemicals

All chemicals were reagent grade. D-sorbitol, D-mannitol, D-glucose, D-galactose, glycerol, Trizma® base (Tris), malic acid, pyruvic acid, citric acid, maleic acid, DL-α-glycerophosphate, NADH, ATP, ADP, rotenone, flavone, antimycin A, propyl-gallate, digitonin, *n*-dodecyl β-D-maltoside (laurylmaltoside), Nitrotetrazolium blue chloride and antifoam A were from Sigma Chem Co. (St Louis, MO). Bovine serum albumin (Probulmin^{TM}) was from Millipore. Yeast extract and bacto-peptone were from BD Bioxon. DL-lactic acid, H_3PO_4, NaCN, KCl, $MgCl_2$ and ethanol were from J.T. Baker. 3,3′-Diaminobenzidine tetrahydrochloride hydrate was from Fluka. Coomassie Blue G was from SERVA (Heidelberg, Germany). Coomassie® brilliant blue G-250 and electrophoresis reagents were from BIO-RAD (Richmond, CA).

2.2. Biologicals

D. hansenii Y7426 strain (US Dept. of Agriculture) was used throughout this work. The strain was maintained in YPGal-NaCl (1% yeast extract, 2% bacto-peptone, 2% D-galactose, 1 M NaCl and 2% bacto-agar) plate cultures. *Yarrowia lipolytica* E150 strain was also used. This strain was maintained in YD (1% yeast extract and 2% D-glucose and 2% bacto-agar) plate cultures.

2.3. Yeast culture and isolation of coupled mitochondria

D. hansenii cells were grown as follows: pre-cultures were prepared inoculating 100 mL of YPLac-NaCl medium (1% yeast extract, 2% bacto-peptone, 2% lactic acid, pH 5.5 adjusted with NaOH and adding NaCl to reach 0.6 M Na^+) containing antifoam A emulsion 50 μL/L. Pre-cultures were grown for 36 h under continuous agitation in an orbital shaker at 250 rpm at 29 °C. Then, each pre-culture was used to inoculate a 750 mL flask with the same medium. Incubation was continued for 24 h (i.e. medium to late logarithmic phase). *D. hansenii* mitochondria were isolated as reported previously [14]. Mitochondria from *Y. lipolytica* were isolated as in [51].

2.4. Protein quantification

Mitochondrial protein was measured by the Biuret method [60]. Absorbance was determined at 540 nm in a Beckman DU-50 spectrophotometer. Bovine serum albumin was used as a standard.

2.5. Oxygen consumption

The rate of oxygen consumption was measured in a YSI-5300 Oxygraph equipped with a Clark-Type electrode (Yellow Springs Instruments Inc., OH) interfaced to a chart recorder. The sample was placed in a water-jacketed chamber at 30 °C. The phosphorylating state (III) was induced with 0.5 mM ADP. The reaction mixture was 1 M sorbitol, 10 mM maleate (pH was adjusted to 6.8 with Tris), 10 mM Tris-phosphate (Pi), 0.5 mM $MgCl_2$ and 75 mM KCl. Mitochondrial protein (Prot) was 0.5 mg/mL; final volume was 1.5 mL. The concentrations of different respiratory substrates and inhibitors are indicated in the legends to the figures.

2.6. Blue native (BN) and 2D SDS-Tricine electrophoresis

BN-PAGE was performed as described in the literature [49]. The mitochondrial pellet was suspended in sample buffer (750 mM aminocaproic acid, 25 mM imidazole (pH 7.0)) and solubilized with 2.0 mg *n*-dodecyl-β-D-maltoside (laurylmaltoside, LM)/mg Prot, or 4.0 mg digitonin (Dig)/mg Prot at 4 °C for 1 h and centrifuged at 33,000 rpm at 4 °C for 25 min. The supernatants were loaded on 4–12% (w/v) polyacrylamide gradient gels. Protein, 0.25 or 0.5 mg per lane was added to 8.5 × 6 cm or 17 × 12 cm gel sizes, respectively. The stacking gel contained 4% (w/v) polyacrylamide. Also, 0.025% digitonin was added to the gel preparation to improve protein band definition [61]. For 2D SDS-Tricine-PAGE, complete lanes from the BN-gels were loaded on 12% polyacrylamide gels to resolve the subunits that constitute each complex. 2D-gels were subjected to Coomassie-staining [61] and silver-staining [62,63]. Apparent molecular weights were estimated using Benchmark Protein (Invitrogen, CA) and Precision Plus Protein^{TM} (BIO-RAD, Richmond, CA) standards.

2.7. In-gel enzymatic activities

In-gel NADH/nitrotetrazolium blue chloride (NTB) oxidoreductase activity was determined incubating native gels in a mixture of 10 mM Tris (pH 7.0), 0.5 mg NTB/mL and 1 mM NADH [64]. Inhibitors such as rotenone and flavone were not able to act on their target enzymes in the gel assays, probably due to dilution into the BN-gel incubation medium, their hydrophobicity or their specific inhibition sites on the protein i.e. the indicator (NTB) seems to receive electrons from flavin prosthetic groups [65], far from the inhibitor blocking sites (near the ubiquinone site) [66,67] (result not shown). In-gel cytochrome *c* oxidase (COX) activity was determined using diaminobenzidine and cytochrome *c* [68]. Cyanide was useful to inhibit COX (Result not shown), but cannot use to unveil the alternative oxidase because there is no method available to measure AOX in-gel activity. In-gel ATPase activity was measured as in [61]. Oligomycin was not able to inhibit this activity (Result not shown) as previously reported in [68].

Table 1
Rates of oxygen consumption in isolated mitochondria from *D. hansenii* in the presence of different respiratory substrates and inhibitors.

Substrate and other additions	Rate of oxygen consumption (natgO · (min · mg Prot)$^{-1}$)	Respiratory control (III/IV)
Pyruvate (10 mM) + malate (10 mM)	123 ± 10*	2.36 ± 0.07
+ADP (500 μM)	290 ± 7**	
+Rotenone (50 μM)	8 ± 1	
+Flavone (500 μM)	114 ± 5	
+Antimycin-A (5 μM)	32 ± 3	
+NaCN (500 μM)	33 ± 2	
+Propyl-gallate (100 μM)	108 ± 6	
Citrate (10 mM) + malate (10 mM)	138 ± 10*	2.17 ± 0.05
+ADP (500 μM)	299 ± 12**	
+Rotenone (50 μM)	11 ± 2	
+Flavone (500 μM)	135 ± 5	
+Antimycin-A (5 μM)	41 ± 3	
+NaCN (500 μM)	39 ± 2	
+Propyl-gallate (100 μM)	128 ± 6	
Succinate (10 mM)	143 ± 11*	1.64 ± 0.08
+ADP (500 μM)	235 ± 14**	
+Rotenone (50 μM)	144 ± 9	
+Flavone (500 μM)	143 ± 11	
+Antimycin-A (5 μM)	38 ± 3	
+NaCN (500 μM)	39 ± 5	
+Propyl-gallate (100 μM)	117 ± 4	
NADH (1 mM)	258 ± 9*	1.23 ± 0.05
+ADP (500 μM)	317 ± 12**	
+Rotenone (50 μM)	243 ± 10	
+Flavone (500 μM)	28 ± 14	
+Antimycin-A (5 μM)	65 ± 3	
+NaCN (500 μM)	65 ± 4	
+Propyl-gallate (100 μM)	204 ± 4	
Glycerol-phosphate (10 mM)	216 ± 10*	1.28 ± 0.03
+ADP (500 μM)	276 ± 11**	
+Rotenone (50 μM)	216 ± 10	
+Flavone (500 μM)	216 ± 10	
+Antimycin-A (5 μM)	39 ± 3	
+NaCN (500 μM)	37 ± 3	
+Propyl-gallate (100 μM)	188 ± 7	

The rates of oxygen consumption were measured in resting state (IV)* and phosphorylating state (III)**. The phosphorylating state was induced with ADP. Rates of oxygen consumption in the presence of inhibitors were measured after a steady state was reached. Reaction mixture: 1 M sorbitol, 75 mM KCl, 10 mM Tris-phosphate, 1 mM $MgCl_2$ and 10 mM maleic acid, pH 6.8 (Tris). Mitochondria 0.5 mg Prot · (mL)$^{-1}$ were added in each assay. Temperature 30 °C. Final volume 1.5 mL. Data from five independent experiments are expressed as the mean ± SD.

2.8. Protein search, alignment and sequence analysis

We used the BLAST website and the NCBI database to search and compare protein sequences from alternative respiratory enzymes. We used the known protein sequences from other yeasts [69–71] to search for possible NDH2s, AOXs and/or $_{Mit}$GPDHs in the *D. hansenii* NCBI database. The identified *D. hansenii* sequences were aligned against those from *S. cerevisiae*, *Y. lipolytica* and/or *C. albicans* using Clustal W 2.0 [72]. The BLAST analysis also indicated the percentages of identity and similarity between amino acid sequences.

2.9. Western blotting

Mitochondrial samples were diluted in 0.5 mL sample buffer (500 mM Tris pH 6.8, 10% glycerol, 10% SDS, 0.05% 2-β-mercaptoethanol and 0.01% bromophenol blue) and boiled for 5 min [73]. SDS-Tricine-PAGE was performed in a 10% polyacrylamide gel. Proteins were electrotransferred to PVDF membranes for immunoblotting using 25 mM potassium phosphate, 25 mM sodium phosphate, 12 mM Tris, 192 mM glycine and 20% methanol, pH 7.0 [74]. Membranes were blocked with 0.5% albumin in TBS/T (50 mM Tris, 100 mM NaCl, pH 7.6, and 0.1% Tween 20) for 1 h and incubated overnight at 4 °C with the primary antibody (monoclonal mouse antibody against the AOX from the higher plant *Sauromatum guttatum* [75]). Then, membranes were washed with TBS/T and incubated at room temperature for 1 h with the horseradish peroxidase (HRP)-conjugated secondary antibody (HRP anti-mouse-igG). Antibodies were diluted in TBS/T. Once the membranes were washed, the bands were developed by chemiluminescence (ECL kit) [76].

2.10. Mass spectrometry

From the BN-gels or 2D SDS-Tricine gels, the indicated bands were excised and sent for protein sequence identification by LC-MS to the University Proteomics Laboratory of the Instituto de Biotecnología, UNAM (Cuernavaca, Morelos, Mexico). Peptides were analyzed in a LC-MS system constituted by an Accela microflux liquid chromatographer (Thermo-Fisher Co., San Jose, CA, USA) with a splitter (1/20), a LTQ Orbitrap Velos mass spectrometer (Thermo-Fisher Co., San Jose, CA, USA) and a nano-electrospray ionization (ESI) system. After tryptic digestion, samples were analyzed in a tandem high-resolution mass spectrometer. Mascot and Protein-Prospector algorithms were used to search all spectrometric results against the NCBInr database. Protein sequence coverage (%) is shown in Tables 3 and 5.

3. Results

3.1. D. hansenii contains a branched mitochondrial respiratory chain

To define the composition of the respiratory chain from *D. hansenii*, we measured the rate of oxygen consumption in isolated mitochondria using different substrates and inhibitors. To prevent the mitochondrial permeability transition (PT), 10 mM phosphate and 75 mM KCl were added (Table 1). As expected [58,59], citrate-malate and pyruvate-malate were efficiently oxidized in a rotenone-sensitive fashion by complex I while succinate was oxidized by complex II. In addition, the complex III inhibitor antimycin-A and the complex IV inhibitor NaCN partially inhibited oxygen consumption. Partial inhibitions indicated the presence of an alternative pathway for oxygen consumption [59]. The presence of an active AOX was confirmed by the partial sensitivity of the rate of oxygen consumption to propyl-gallate (PG). PG was preferred over salicylhydroxamic acid (SHAM) because full inhibition was achieved with 100 μM PG while a higher 500 μM SHAM was needed (Result not shown). Full inhibition of oxygen consumption was achieved by adding NaCN and PG together (Table 1).

The above results confirm the presence of a branched mitochondrial respiratory chain in *D. hansenii* that contains at least all four multisubunit complexes plus an alternative AOX [55,56]. The presence of additional external alternative dehydrogenases was suggested when NADH and glycerol-phosphate were oxidized at high rates (Table 1). Oxidation of these substrates was partially sensitive to both, NaCN or PG, indicating that electrons coming from these substrates could reach either the cytochrome pathway or AOX. The external NADH dehydrogenase (NDH2e) activity was sensitive to flavone, a specific inhibitor of type II NADH dehydrogenases, but it was not sensitive to rotenone. Also, the glycerol-phosphate dehydrogenase ($_{Mit}$GPDH) activity was not sensitive to either rotenone or flavone. Thus, it is suggested that *D. hansenii* contains a branched mitochondrial respiratory chain composed by the four canonical complexes, alternative dehydrogenases (at least NDH2 and $_{Mit}$GPDH) and an AOX.

The substrates predicted to yield a higher number of protons-pumped per electron consumed in the respiratory chain (H^+/e^-) exhibited a higher respiratory control (RC = phosphorylating state (III)/resting state (IV)) than those with a low H^+/e^- (Table 1), i.e., the highest respiratory controls were obtained using pyruvate-malate, RC = 2.35 ± 0.07 or citrate-malate, RC = 2.17 ± 0.05. By contrast,

with succinate a low RC = 1.64 ± 0.08 was observed, while with glycerol-phosphate RC = 1.28 ± 0.03 and with NADH RC = 1.23 ± 0.05.

3.2. The putative mitochondrial NDH2e from D. hansenii is inhibited by flavone and exhibits a high homology with NDH2s from other sources

To confirm the presence of external NDH2(s) in *D. hansenii* the rate of oxygen consumption was titrated with rotenone to inhibit complex I or flavone to inhibit any NDH2 activity present [38]. The rate of oxygen consumption in the absence of inhibitors was taken as 100%. In the presence of pyruvate-malate, respiration was inhibited by rotenone, but it was insensitive to flavone (Fig. 1A). At 5 μM rotenone 50% inhibition was obtained while maximum inhibition of the pyruvate-malate-supported oxygen consumption was reached at 50 μM rotenone (Fig. 1A, full circles). By contrast, with NADH, flavone inhibited oxygen consumption while rotenone exhibited little effect (Fig. 1B). In the presence of NADH, 500 μM flavone led to maximal inhibition (Fig. 1B, empty circles).

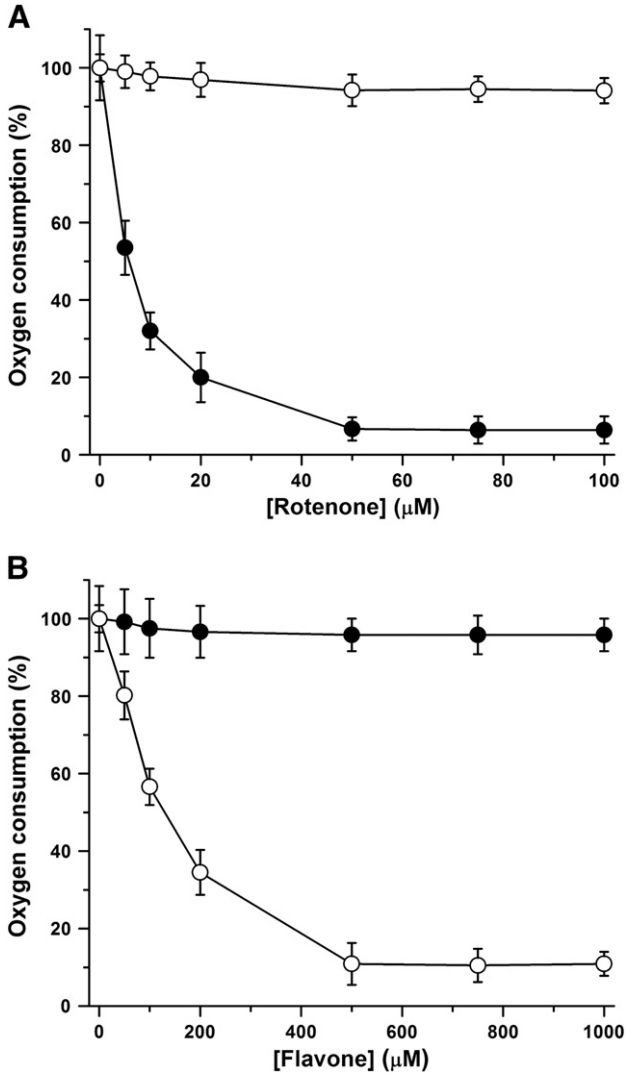

Fig. 1. Inhibition of oxygen consumption in isolated mitochondria from *D. hansenii* with rotenone (A) or flavone (B). The substrate was either 10 mM pyruvate-malate (●) or 1 mM NADH (○). Oxygen measurements were made in the resting state (IV). The reaction mixture was as in Table 1. Data from five independent experiments are expressed as the mean ± SD.

Yeast species may contain different alternative dehydrogenases, e.g. *S. cerevisiae* contains three mitochondrial NDH2 isoforms plus an external $_{Mit}$GPDH [21,40]. To detect possible alternative dehydrogenases in the NCBI database, the genome of *D. hansenii* was analyzed for sequences homologous to those encoding for NDH2s and $_{Mit}$GPDHs in *Y. lipolytica* and *S. cerevisiae*. For NDH2s, the BLAST analysis unveiled a protein sequence with high homology to type II NADH dehydrogenases. This is the hypothetical protein DEHA2D07568p, a 568 amino acid (MW = 63 kDa) precursor. DEHA2D07568p was aligned against the NDH2e sequence from *Y. lipolytica* (YALI0F25135p) and the NDH2s from *S. cerevisiae*, i.e. NDI (YML120c), NDE1 (YMR145c) and NDE2 (YDL085w) (Table 2), exhibiting high sequence similarity. In addition, DEHA2D07568p closely resembles external NDH2s from several fungi and plants (Result not shown). Furthermore, when the conserved motifs described for the NDH2e from *Y. lipolytica* [77] were compared with the DEHA2D07568p, both proteins exhibited highly matching dinucleotide binding sites (for NADH or FAD) and hydrophobic regions (Fig. 2). These results plus the flavone sensitivity strongly suggest that DEHA2D07568p is an NDH2e. In addition, there is a 98.9% probability that this protein is imported into mitochondria as predicted by the MitoProt II-v1.101 program [78]. Analysis of the *D. hansenii* genome did not detect other genes coding for NDH2s.

3.3. D. hansenii has a mitochondrial glycerol-phosphate dehydrogenase ($_{Mit}$GPDH)

Isolated mitochondria from *D. hansenii* oxidized glycerol-phosphate at a high rate (Table 1), suggesting the presence of a mitochondrial GPDH as predicted by Adler and co-workers [79]. Thus, to look for orthologues the *D. hansenii* sequences were aligned against the corresponding genes from *S. cerevisiae* (Gut2p) and *Y. lipolytica* (YALI0B13970p). The analysis unveiled only one candidate sequence, annotated as hypothetical protein DEHA2E08624p; a 652 amino-acid precursor, MW = 72.5 kDa with a 65.9% probability of being imported by mitochondria [78]. DEHA2E08624p sequence is similar to $_{Mit}$GPDHs from other yeast species (Table 2) and with other $_{Mit}$GPDHs stored in the NCBI database. Thus, our data suggest that DEHA2E08624p is a mitochondrial GPDH.

3.4. The AOX in D. hansenii mitochondria is sensitive to AMP

In isolated mitochondria from *D. hansenii* cyanide-resistant respiration (CRR) was ~20–25% of the total. In different organisms this percentage can vary depending on different molecules or environmental

Table 2
D. hansenii putative alternative oxidoreductase sequences. Percentage of identity and similarity with those from other yeast sources.

Sequences	Identity (%)	Similarity (%)
a) NDH2s		
• DEHA2D07568p vs. YALI0F25135p (*Yl*NDH2e)	50	65
• DEHA2D07568p vs. YML120c (*Sc*NDE1)	45	64
• DEHA2D07568p vs. YMR145c (*Sc*NDE2)	52	69
• DEHA2D07568p vs. YDL085w (*Sc*NDI)	50	69
b) $_{Mit}$GPDHs		
• DEHA2E08624p vs. YALI0B13970p (Yl_{Mit}GPDH)	49	64
• DEHA2E08624p vs. Gut2p (Sc_{Mit}GPDH)	58	73
c) AOXs		
• DEHA2C03828p vs. AAQ08895 (*Yl*AOX1)	54	69
• DEHA2C03828p vs. AAQ08896 (*Yl*AOX2)	50	66
• DEHA2C03828p vs. XP_723460 (*Ca*AOX1)	63	73
• DEHA2C03828p vs. XP_723269 (*Ca*AOX2)	65	79

Protein sequences are shown accordingly with their NCBI definition or accession nomenclature.
Abbreviations: *Sc*: *S. cerevisiae*; *Yl*: *Y. lipolytica*; *Ca*: *C. albicans*; NDH2e/NDE: external alternative NADH dehydrogenase; NDI: internal alternative NADH dehydrogenase; AOX1: alternative oxidase isoform 1; AOX2: alternative oxidase isoform 2; Mit: mitochondrial isoform.

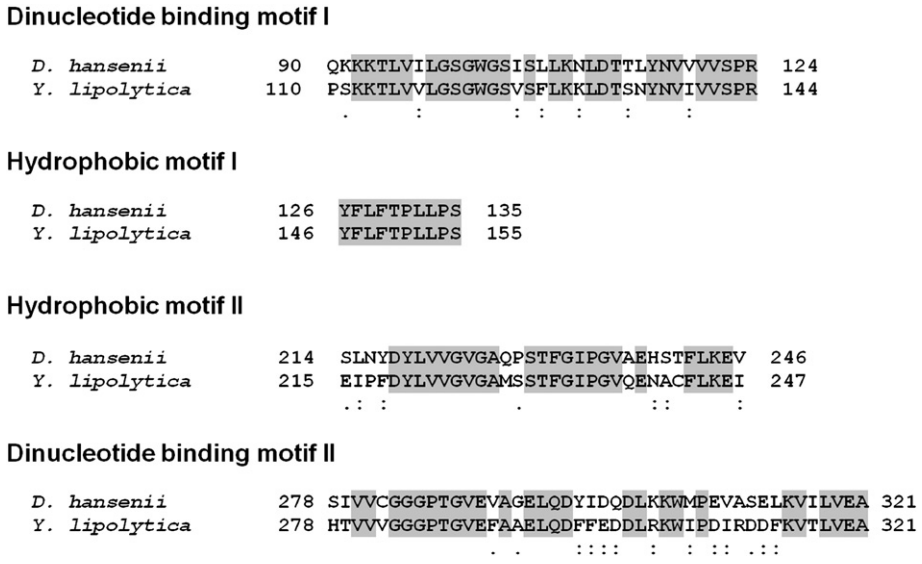

Fig. 2. Alignment of the conserved motifs of DEHA2D07568p and *Y. lipolytica* NDH2e amino acid sequences. (:) Conserved substitutions; (.) semi-conserved substitutions. Identical residues in both sequences are shown in gray. Numbers indicate amino acids in the linear sequence of each protein.

conditions, e.g. α-ketoacids, AMP, salts, temperature and mitochondrial-matrix redox state [80–82]. In addition, many plants and microorganisms express AOX in response to ROS or cytochromic pathway inhibitors [83,84]. AOXs from yeast or from *Ustilago maydis* are activated by AMP and possibly by the redox state, but not by α-ketoacids [85]. To test some of the properties of the *D. hansenii* AOX ($_{Dh}$AOX); it was decided to explore the sensitivity to AMP or pyruvate. To measure only CRR, these experiments were conducted in the presence of 500 μM NaCN. Full oxygen consumption inhibition was achieved with 500 μM NaCN plus 100 μM propyl-gallate. It was observed that AMP increased CRR (~15%) while pyruvate had no effects (Fig. 3), i.e. the AOX from *D. hansenii* shares the sensitivity to AMP from other fungi AOXs.

Further analysis of AOX was conducted by comparing the $_{Dh}$AOX hypothetical protein sequence with the constitutive and inducible AOX isoforms (1 and 2, respectively) from *Yarrowia lipolytica* and *Candida albicans*. The BLAST analysis unveiled only one candidate, annotated as hypothetical protein DEHA2C03828p. This sequence corresponds to a 338 amino-acid precursor with a theoretical MW of 39.4 kDa. There is a 97.1% probability that this protein is imported by mitochondria [78]. The DEHA2C03828p sequence has high similarity to the AOXs from both yeast species (Table 2). With the above results, it may be concluded that *D. hansenii* mitochondria contain a branched respiratory chain composed by all four canonical complexes plus three alternative oxido-reductases, namely an NDH2e, a $_{Mit}$GPDH and the $_{Dh}$AOX already reported [59]. Alternative enzymes were analyzed using SDS-Tricine PAGE, western blotting and mass spectrometry (see below).

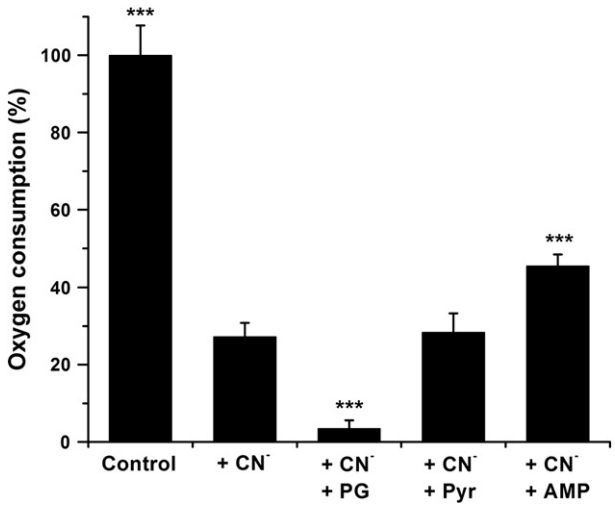

Fig. 3. Activation of the *D. hansenii* AOX by AMP but not by pyruvate (Pyr). Oxygen consumption was measured in state IV with 10 mM succinate as respiratory substrate. 50 μM rotenone was added to inhibit complex I. Cytochrome-dependent oxygen consumption was inhibited with 500 μM NaCN (CN^-). 100 μM propylgallate (PG), 10 mM pyruvate (Pyr) or 1 mM AMP was used as indicated. n = 3 ± SD. One-way ANOVA (Dunnett's multiple comparison test) *P < 0.05 compared to the cyanide-treated sample (second bar).

3.5. In *D. hansenii* mitochondria, respiratory complexes organize into supercomplexes

After detection of the different components of the mitochondrial respiratory chain from *D. hansenii*, it was decided to define whether the respiratory complexes were organized into supercomplexes as described for many other species [48,50,51]. Both *D. hansenii* and *Y. lipolytica* are closely related [69,70], so we decided to use *Y. lipolytica* mitochondrial respiratory complexes and supercomplexes as standards to estimate the MW of those from *D. hansenii*. For BN-PAGE, mitochondrial membranes were solubilized with either laurylmaltoside (LM) or digitonin (Dig). Digitonin was used expecting to preserve associations between respiratory complexes, while laurylmaltoside was expected to allow isolation of the individual complexes. The BN-PAGE results are shown for solubilized mitochondria from *Y. lipolytica* (Fig. 4A) and from *D. hansenii* (Fig. 4B). In LM-solubilized mitochondria, the individual complexes from either *Y. lipolytica* or *D. hansenii* were observed at different migration distances. Migration distances for complexes I, IV and V were reasonably near in both species. By contrast, the complex III band from *D. hansenii* was hardly detectable by BN-PAGE (Fig. 4B lane LM). In fact, the location of complex III was detected only in the 2D Tricine-SDS-PAGE (see below). In digitonin-solubilized mitochondria from both *Y. lipolytica* (Fig. 4A) and *D. hansenii* (Fig. 4B) several high MW bands corresponding to putative respiratory supercomplexes were revealed.

To further characterize the location and composition of each complex and supercomplex, the in-gel enzymatic activities of NADH dehydrogenase (NDH), ATPase and cytochrome *c* oxidase (COX) were assayed in BN-gels (Fig. 4C to E). In the LM solubilized sample, NDH activity

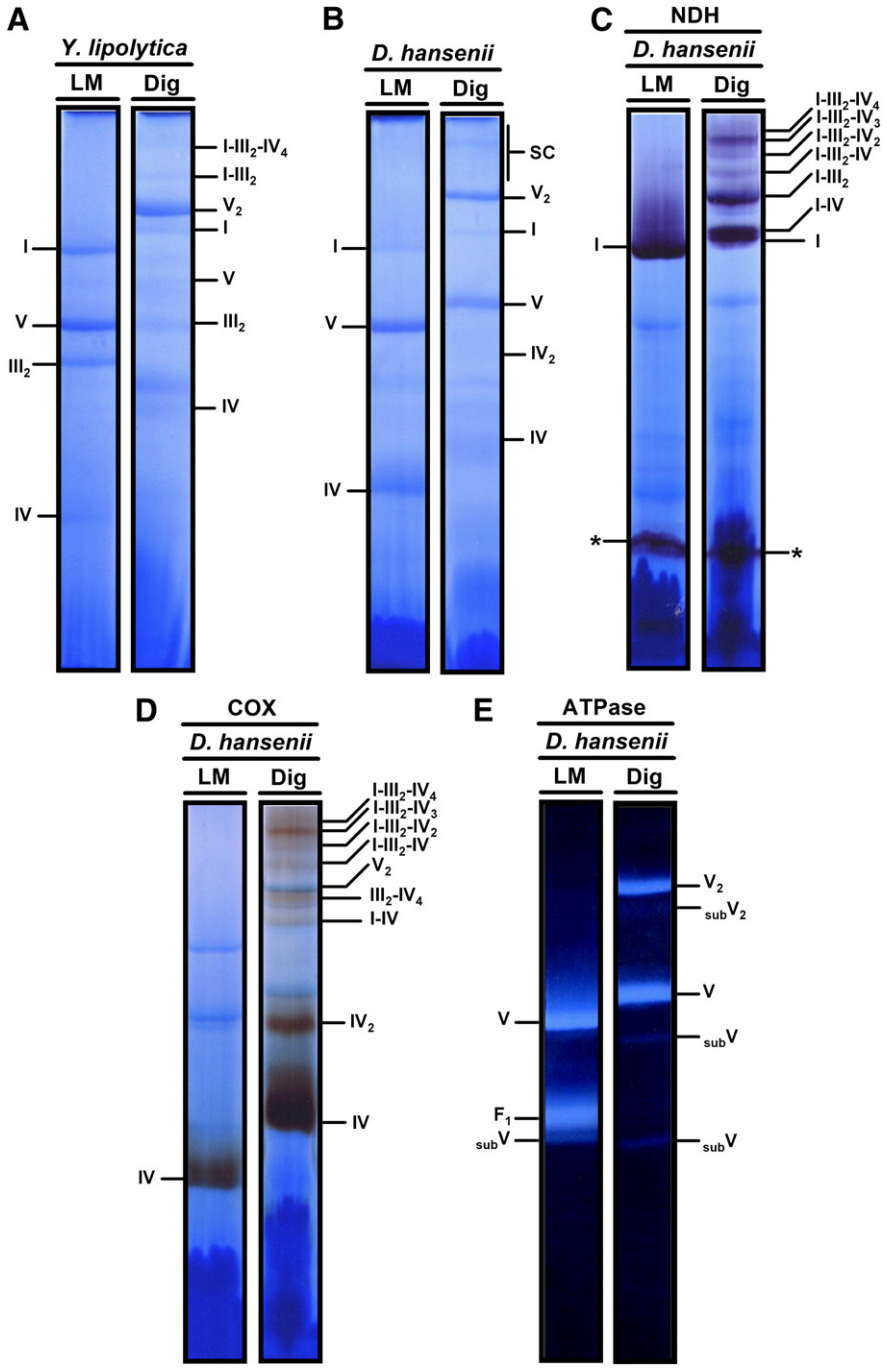

Fig. 4. Respiratory complexes and supercomplexes found in solubilized *D. hansenii* mitochondria. Isolated mitochondria were solubilized with laurylmaltoside (LM) 2.0 mg/mg Prot or digitonin (Dig) 4.0 mg/mg Prot. (A) *Y. lipolytica* solubilizates were resolved by BN-PAGE in a 4–12% polyacrylamide gradient gel and were used as MWs standards. (B) LM- and Dig-solubilizates from *D. hansenii* mitochondria resolved by BN-PAGE. (C) In-gel NADH-dehydrogenase activity (NDH); 1 mM NADH and 0.5 mg/mL nitrotetrazolium blue chloride (NTB). (D) In-gel cytochrome *c* oxidase activity (COX); 0.04% diaminobenzidine and 0.02% cytochrome *c*. (E) In-gel ATPase activity performed in BN-gel; 35 mM Tris, 270 mM glycine, 0.2% $Pb(NO_3)_2$, 14 mM $MgSO_4$ and 8 mM ATP (pH 8.4). I, III_2, IV and V are the mitochondrial mammalian-like complexes. (*) Putative NDH2e. *D. hansenii* supercomplexes (SC) were: I–IV, I–III_2, I–III_2–IV, I–III_2–IV_2, I–III_2–IV_3 and I–III_2–IV_4 where stoichiometries are indicated as sub-indexes. IV_2: complex IV dimer; F_1: soluble domain of complex V; V_2: complex V dimer; subV: complex V sub-complexes.

exhibited two purple bands corresponding to complex I and presumably to the NDH2e (Fig. 4C lane LM). When solubilized with digitonin, higher MW purple bands were detected (Fig. 4C lane Dig). These bands were assigned as supercomplexes containing complex I plus different amounts of either complex III or complex IV (see below). Also, the NDH activity seemed more intense in three bands than in all others, suggesting that complex I-containing supercomplexes were concentrated in these bands. These bands had MWs compatible with their assignment as the complex I band running alone; as a I-IV supercomplex; a I-III_2 supercomplex and a I–III_2–IV_3 supercomplex (Fig. 4C lane Dig; also see Fig. 4D which is described below).

When COX activity was measured, a single brown band was observed in the LM-solubilized lane (Fig. 4D lane LM). It is suggested that this activity is the product of monomeric complex IV. The digitonin lane revealed several brown bands corresponding to monomeric complex IV and to a number of supercomplexes containing complexes I, III_2

and IV (Fig. 4D lane Dig). Supercomplex I-III_2-IV_3 exhibited the highest activity. Also, a faint band, probably corresponding to I–IV supercomplex was detected near complex I.

In regard to in-gel ATPase activity, LM treatment revealed three activity bands that were respectively assigned as the monomeric complex V, the F_1 subunit and a F_1 subcomplex (Fig. 4E lane LM). In the first two bands the ATPase activity was much higher than the activity detected in the subcomplex, indicating that this may be at low concentrations or exhibit less activity. In the digitonin solubilized samples ATPase activity was detected in four bands (Fig. 4E lane Dig). The ATPase activity was more intense in the bands assigned as the complex V dimer and monomer, while the lower intensity bands probably were the F_1 subunit and an F_1F_O-ATP synthase sub-complex. Dimers of complex V have also been detected previously in mitochondria from beef heart, *S. cerevisiae*, *Polytomella* sp. and from other sources by digitonin solubilization or using lower LM/protein ratios [51].

To determine the location of each respiratory complex, including complex III which was not observed in the BN gels, and also whether any given complex was part of a putative supercomplex, complete BN-PAGE lanes from LM- and Dig-solubilized mitochondria were resolved by second dimension denaturing gels (2D Tricine-SDS-PAGE) and subjected to Coomassie-staining (Fig. 5) or silver-staining (Fig. 6), respectively. The second dimension gel from LM-solubilized mitochondria contains the individual subunit signatures [49] from each respiratory complex (Fig. 5). In order to confirm the assignments for complexes I, III, IV and V different bands were excised and sent to protein identification by LC-MS. The 75-kDa subunit from NADH dehydrogenase (I), the core proteins 1 and 2 from the bc_1 complex (III), the COX subunit 2 from cytochrome *c* oxidase (IV) and the gamma (γ) subunit from F_1F_O-ATP synthase (V) were identified with a high sequence coverage (Table 3). In all cases, identified subunits were located at the lane that was previously predicted for a specific respiratory complex. Complex III, which was difficult to see before (Fig 4B, lane LM), could be located next to the complex V monomer (Fig. 5).

In the 2D-gel obtained from digitonin-solubilized mitochondria, the subunit pattern of individual complexes was found also at high MWs indicating the presence of supercomplexes (Fig. 6). The MWs suggested that these supercomplexes contained complexes I, III and IV. In addition, a pattern corresponding to a complex V dimer (V_2) was identified. It is suggested that the supercomplexes detected by BN-gels (Fig. 4) and 2D SDS-Tricine-gels (Figs. 5 and 6) were: IV_2, I–IV, III_2–IV_4, V_2, I-III_2 (S_0), I–III_2–IV (S_1), I–III_2–IV_2 (S_2), I–III_2–IV_3 (S_3) and I–III_2–IV_4 (S_4).

To determine the stoichiometry and the theoretical MWs of these supercomplexes, the MWs of each complex/supercomplex were estimated by measuring the migration distance of the corresponding bands in BN-PAGE of the digitonin solubilizates from *D. hansenii* and interpolating them by linear regression in a log MW vs. migration distance plot from the solubilized mitochondrial respiratory complexes from *Y. lipolytica* that we used as MW standards (Fig. 7). The estimated MWs are shown in Table 4. The composition of each supercomplex was determined by correlating the MW estimates and the presence of NDH, COX and/or ATPase activity in each band. The calculated MWs for complex I, IV and V monomers and complex III dimer were very similar to those from *Y. lipolytica* (Fig. 7). The *D. hansenii* MWs of the supercomplexes were similar to those reported for *Y. lipolytica* [51]. By contrast, the complex V dimers from *D. hansenii* were heavier than expected (Table 4).

In mammalian systems, large supercomplexes containing I_1–III_2–IV_4 and III_2–IV_4 have been detected in BN-gels [49]. Also, mammalian supercomplexes seem to be associated into larger "respiratory strings" [86]. In *D. hansenii*, it seems that complexes I, III_2 and IV organize into supercomplexes suggesting that these mitochondria also possess "respiratory strings" where chain units of the I–III_2–IV_3 supercomplex would attach to each other. In contrast to *Y. lipolytica* [87], NDH2e seems to be detached from the cytochrome-complexes; i.e. in digitonin-treated samples in-gel NADH dehydrogenase activity was absent at the sites where cytochrome complexes migrated (Fig. 4C lane Dig).

At this point, we can conclude that the branched respiratory chain from *D. hansenii* contains a large amount of canonical respiratory complexes (I, III and IV), which may be associated in supercomplexes (Fig. 4). Alternative enzymes probably are independent from the respiratory supercomplexes (at least the NDH2e (Fig. 4C lane Dig). Nevertheless alternative enzyme distribution needs to be explored further.

3.6. Identification of the alternative respiratory enzymes from D. hansenii

NDH2e has already been proposed to correspond to the lower NADH dehydrogenase activity band detected in a BN-gel (Fig. 4C); when this band was subjected to 2D-SDS-Tricine-PAGE different proteins were separated (Fig. 8). Three spots were selected for identification; the

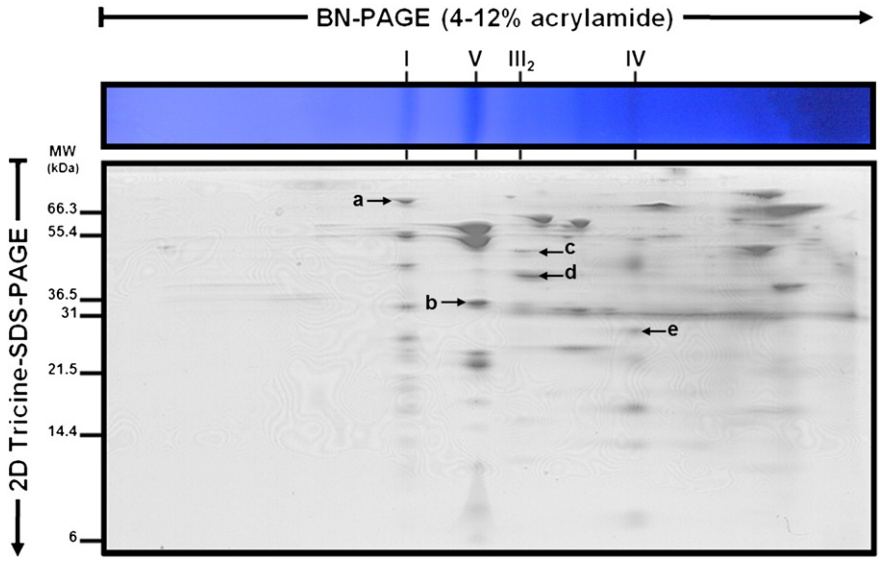

Fig. 5. 2D SDS-Tricine-PAGE of *D. hansenii* mitochondrial respiratory complexes. From the BN-PAGE, the lane containing the laurylmaltoside (LM) solubilized proteins was excised and subjected to 2D SDS-Tricine-PAGE. Bands that appear labeled were cut and sent for protein identification by LC-MS. These results are shown in Table 3. All SDS-Tricine-gels showed were stained with Coomassie® brilliant blue G-250. Respiratory complexes are tagged as in Fig. 4.

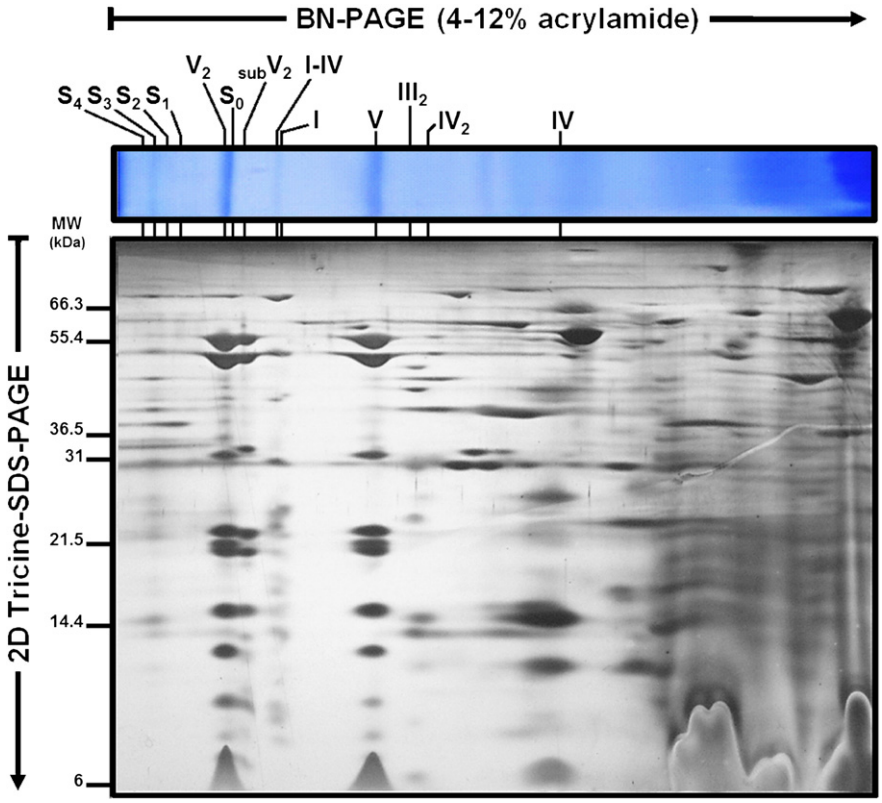

Fig. 6. 2D SDS-Tricine-PAGE of *D. hansenii* mitochondrial supercomplexes. After BN-PAGE, the lane containing the digitonin-solubilized proteins was excised and subjected to 2D-SDS-Tricine-PAGE followed by silver staining. Respiratory complexes are tagged as in Fig. 4. Supercomplex nomenclature: S_0: I–III_2, S_1: I–III_2–IV, S_2: I–III_2–IV_2, S_3: I–III_2–IV_3 and S_4: I–III_2–IV_4.

first corresponded to the hypothetical MW of NDH2e; i.e. 63 kDa (Fig. 8, f) and the other two were chosen due to their high concentration (Fig. 8, bands g and h). The spots were analyzed by LC-MS/MS and the results are shown in Table 5. The first band (f) was reported as the NDH2e hypothetical sequence (DEHA2D07568p) but surprisingly, it also contained the putative $_{Mit}$GPDH (DEHA2E08624p), in spite that the predicted MWs were widely different (63 vs. 72.5 kDa, respectively) (Table 5), i.e. they were in the same spot in the 2D SDS-Tricine-gel (Fig. 8). The presence of both proteins in the asterisked band (excised from the BN-gel, Fig. 4) might reflect a physiological interaction of these alternative dehydrogenases. A similar interaction has been described in *S. cerevisiae* as part of a mitochondrial dehydrogenase membrane complex, which contains different external peripheral alternative dehydrogenases, part of the Krebs cycle enzymes (including complex II), the NDI and other NADH producing enzymes that were not defined [88]. Also, in *D. hansenii* dihydrolipoamide dehydrogenase was identified next to NDH2e and $_{Mit}$GPDH (Fig. 8, g). This protein is part of the pyruvate dehydrogenase and the α-ketoglutarate dehydrogenase complexes [20]. The lower band contained three proteins: the ATP/ADP carrier (ANC); the mitochondrial porin (VDAC) and the phosphate carrier (Fig. 8, h). These proteins are involved in metabolite fluxes and have been proposed to be part of the mitochondrial unspecific channel in other yeast species [89].

In *S. cerevisiae* $_{Mit}$GPDH (Gut2p) has a predicted MW = 72.4 kDa, while the mature form of this protein has a MW = 68.4 kDa [88]. This MW is close to the mature *S. cerevisiae* NDE2 with a MW = 61.7 kDa [88]. In *D. hansenii*, NDH2e exhibited an approximate MW = 60 kDa (Fig. 8) and $_{Mit}$GPDH migrated very near that weight. In silico data and estimated MWs suggested that *D. hansenii* $_{Mit}$GPDH contains a longer signal-sequence than the NDH2e. When both proteins maturate, their MWs become similar and their electrophoretic migration coincides. As a result, both dehydrogenases appeared in the same 2D-gel spot (Fig. 8, f; Table 5).

AOX was identified by mass spectrometry (Fig. 9, upper panel) and by western blotting (WB) (Fig. 9, lower panel). For the western blot, an antibody against AOX from *S. guttatum* was used. Two bands were detected by this procedure (Fig. 9, lower panel). To determine which of these bands contains AOX, they were excised from the gel and sent

Table 3
Proteins identified by LC-MS analysis contained in the indicated bands from the 2D SDS-Tricine-gel (Fig. 5).

Band	Protein name	Accession no.	gI protein	Length[a]	Cov[b] (%)	MW[c] (kDa)
a	NADH-quinone oxidoreductase 75-kDa subunit	DEHA2G06050p	199433960	722	26.7	79
b	F_1F_0-ATP synthase gamma subunit	DEHA2F20658p	202953475	286	36.7	31.3
c	Ubiquinol-cytochrome *c* reductase core protein 1	DEHA2D13640p	199431718	445	31.7	48
d	Ubiquinol-cytochrome *c* reductase core protein 2	DEHA2E09834p	49655402	376	75	39.4
	IDH2 subunit of mitochondrial NAD(+)-dependent isocitrate dehydrogenase	DEHA2G05786p	49657467	365	22.2	39.5
	IDH1 subunit of mitochondrial NAD(+)-dependent isocitrate dehydrogenase	DEHA2C10758p	199430720	359	19.2	38.6
e	Cytochrome *c* oxidase subunit 2	YP_001621413.1	162951843	246	11.7	28.4

[a] Number of amino acids.
[b] Protein sequence coverage.
[c] Predicted molecular weights from the *D. hansenii* NCBI database sequences.

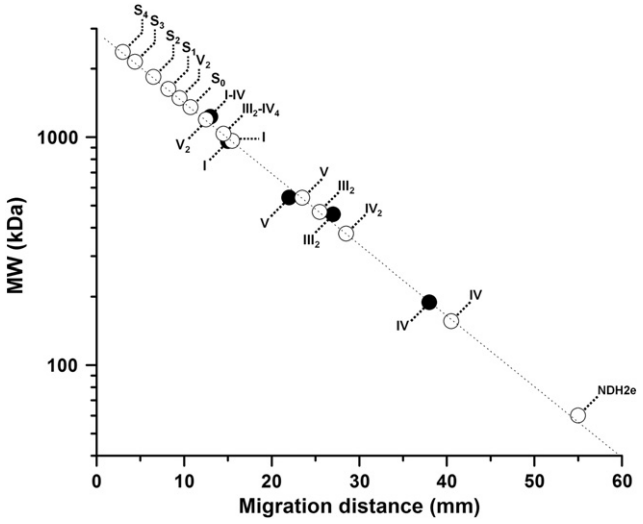

Fig. 7. Molecular weight (MW) estimates of the *D. hansenii* complexes and supercomplexes. The previously characterized molecular masses of *Y. lipolytica* mitochondrial complexes were plotted against their migration distance in BN-PAGE (●). Then, the migration distances of the *D. hansenii* respiratory complexes and supercomplexes (○) were interpolated and their corresponding molecular masses inferred (see values in Table 4). MW values from *Y. lipolytica* complexes I, III_2, IV, V and complex V dimer (V_2) were taken from the previous report by Guerrero-Castillo and co-workers [51]. (*) Putative NDH2e. Note that *y*-axis is in log-scale. Nomenclature for complexes and supercomplexes is as in Figs. 4 and 6.

to LC-MS/MS analysis. AOX was the "i" band (Fig. 9, upper panel) while the "j" band contained the ANC and VDAC (Fig. 9, upper panel). Results are shown in Table 5.

Experimental evidence supports the presence of a branched mitochondrial respiratory chain in *D. hansenii*. This chain contains the multi-subunit complexes I, II, III and IV; there is also a mitochondrial F_1F_O-ATP synthase (complex V), which tends to be a dimer and is detached from the respiratory supercomplexes (Fig. 4E). Three alternative enzymes: NDH2e, $_{Mit}$GPDH and $_{Dh}$AOX were detected as additional components of the branched respiratory chain. Preliminary evidence presented here suggests that multiprotein associations containing the alternative dehydrogenases plus at least two enzymes from the Krebs cycle do exist. Such associations have been described in *S. cerevisiae* [88].

Table 4
Estimated molecular weights (MWs) of the *D. hansenii* complexes and supercomplexes by BN-PAGE.

Complex/supercomplex	Calculated MW[a] (kDa)	Expected MW[b] (kDa)
I	963 ± 49	–
III_2	469 ± 24	–
IV	156 ± 12	–
V	541 ± 28	–
IV_2	377 ± 19	312
I–IV	1035 ± 53	1119
III_2–IV_4	1196 ± 61	1223
I–III_2 (S_0)	1356 ± 35	1432
V_2	1484 ± 76	1082
I–III_2–IV (S_1)	1630 ± 87	1588
I–III_2–IV_2 (S_2)	1842 ± 51	1744
I–III_2–IV_3 (S_3)	2143 ± 59	1900
I–III_2–IV_4 (S_4)	2370 ± 135	2056

Complex and supercomplex nomenclature as in Figs. 4–6.
[a] Calculated MW of the *D. hansenii* complexes and supercomplexes correspond to the mean ± SD from three independent experiments.
[b] Supercomplexes expected MWs correspond to the sum of the individual MW of each respiratory complex according to their stoichiometries (subscript numbers).

4. Discussion

The structure of the branched mitochondrial respiratory chain from *D. hansenii* was analyzed in isolated mitochondria. In addition, we characterized the association pattern of respiratory complexes into respiratory supercomplexes [44,48,49,86]. In agreement with Veiga and co-workers [59], we found that the *D. hansenii* respiratory chain contains all four canonical respiratory complexes I, II, III and IV plus an AOX. In addition, we detected two additional components, namely, an external type II NADH dehydrogenase (NDH2e) and a mitochondrial glycerol-phosphate dehydrogenase ($_{Mit}$GPDH).

AOX activity is resistant to cyanide [58,80]; electrons reach it directly from the ubiquinone pool, as indicated by the resistance of oxygen consumption activity to the complex III inhibitor antimycin-A (Table 1, Fig. 3). Cyanide-resistant, AOX-supported respiration is found in many yeast species, including *D. hansenii* and it has been proposed that AOX regulates energy production in response to different physiological conditions [57–59]. Regulation is the result of a decrease in the electron flux to the cytochromic pathway with the concomitant increase in electron flux to AOX [34–36,87]. Here, it was observed that *D. hansenii* alternative oxidase ($_{Dh}$AOX) is activated by AMP while it is insensitive to α-ketoacids, such as pyruvate. AMP activation is widely reported for AOXs from different yeasts and fungi [21,80,85]. It was suggested that $_{Dh}$AOX activity is induced at the stationary growth phase [59]. In this view, the presence of the AOX could be helpful to diminish the electron flux through the cytochromic pathway and reduce the ATP/O ratio in this physiological condition. In contrast to Veiga and co-workers [59], in our hands $_{Dh}$AOX activity was detected in isolated mitochondria from mid-exponential growth phase cultures. This is probably due to the differences in growth conditions, as we used a non-fermentable carbon source (lactate, see Materials and methods) [14]. This result suggests that $_{Dh}$AOX is active in early growth phases and not only at the stationary phase where it probably acts as an energy sink [35,87]. In cells grown in lactate, $_{Dh}$AOX was detected regardless of the addition of AMP (Table 1, Fig. 3). The role of $_{Dh}$AOX in different growth phases requires further studies.

Two other alternative enzymes, a glycerol-phosphate dehydrogenase and an alternative NADH dehydrogenase were both bound to the external face of the IMM. Electrons were fed to $_{Mit}$GDPH and NDH2e by external glycerol-phosphate or NADH, respectively. These electrons were used to reduce oxygen. From the BLAST analysis of the genomes, we concluded that there is a single gene codifying for each of these

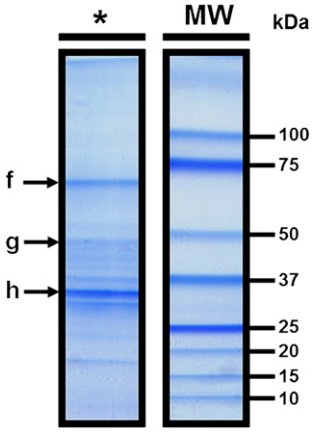

Fig. 8. Identification of the *D. hansenii* alternative NADH dehydrogenase (NDH2e) and the mitochondrial glycerol-posphate dehydrogenase ($_{Mit}$GPDH) by 2D SDS-Tricine-PAGE and LC-MS. (*) NADH dehydrogenase activity band from the BN gel, which was excised and subjected to 2D SDS-Tricine-PAGE in order to separate components. SDS-Tricine-gel was stained with Coomassie® brilliant blue G-250. Both *D. hansenii*. Bands contained f: NDH2e and MitGPDH, g: dihydrolipoamide dehydrogenase (subunit from pyruvate dehydrogenase and α-keto glutarate dehydrogenase) and h: ANC, PiC and VDAC (Table 5).

Table 5
Proteins identified by LC-MS analysis contained in the indicated bands from the SDS-Tricine-gels (Figs. 8 and 9).

Band	Protein name	Accession no.	gI protein	Length[a]	Cov[b] (%)	MW[c] (kDa)
f	Glycerol-3-phosphate dehydrogenase ($_{Mit}$GPDH) precursor	DEHA2E08624p	49655350	652	25.3	72.5
	Mitochondrial external alternative NADH dehydrogenase (NDH2e) precursor	DEHA2D07568p	199431532	568	38.2	63
g	Dihydrolipoamide dehydrogenase	CBS767	49653406	495	58	53.2
h	Major ADP/ATP carrier (ANC) of the mitochondrial inner membrane	DEHA2E12276p	49655508	301	41.5	33
	Voltage-dependent anion channel (VDAC) of the outer mitochondrial membrane	DEHA2D16456p	49654868	282	65.6	29.9
	Mitochondrial phosphate carrier (PiC)	DEHA2B12188p	49653149	307	33.6	32.4
i	Alternative oxidase (AOX) precursor	DEHA2C03828p	199430515	338	36.7	39.4
j	Major ADP/ATP carrier (ANC) of the mitochondrial inner membrane	DEHA2E12276p	49655508	301	38.5	33
	Voltage-dependent anion channel (VDAC) of the outer mitochondrial membrane	DEHA2D16456p	49654868	282	52.1	29.9

[a] Amino acid sequence length.
[b] Protein sequence coverage.
[c] Predicted molecular weights from the *D. hansenii* NCBI database sequences.

proteins and we assigned DEHA2E08624p and DEHA2D07568p as the $_{Mit}$GPDH and the NDH2e, respectively. These sequences were highly homologous to those from *Y. lipolytica* [77] and *S. cerevisiae* [90] (Fig. 2, Table 2).

NDH2e from *D. hansenii* was insensitive to rotenone while it was inhibited specifically by flavone. In isolated mitochondria from *D. hansenii*, 500 μM flavone promoted maximum inhibition of oxygen consumption (Fig. 1B, empty circles), which is similar to the concentrations reported for other organisms, e.g. in isolated mitochondria from *Plasmodium yoelii yoelii* [91] or *Paracoccidioides brasiliensis* [92] exogenous NADH-supported oxygen uptake is inhibited at similar flavone concentrations. In isolated mitochondria from *U. maydis*, complete inhibition is obtained at 250 μM flavone [85]. The flavone-mediated inhibition of the NADH:Q_6 oxidoreductase from *S. cerevisiae* exhibited an IC_{50} = 95 μM, although in the presence of 300 μM flavone, activity was still at 20% [38].

NDH2e has been proposed to compensate for the absence of an aspartate-malate shuttle in ascomycetous fungi [85]. Here, we observed a high rate of exogenous NADH oxidation in isolated mitochondria from *D. hansenii*. Mitochondrial NADH oxidation probably occurs in the intact cell, establishing a NADH/NAD^+ recirculation cycle with the cytosol. Furthermore, probably $_{Mit}$GPDH also constitutes an important mitochondrial sink of redox equivalents [93].

In *D. hansenii* active synthesis and accumulation of glycerol and lipids occur during growth; remarkably, these activities are stimulated by high salt concentrations [79] and $_{Mit}$GPDH seems to participate in both processes. In addition, in *S. cerevisiae*, glycerol-phosphate dehydrogenase is finely regulated by the activity of NDHs, i.e. at saturating NADH, alternative NADH dehydrogenases physically attached to the $_{Mit}$GPDH inhibit the use of glycerol-phosphate and transfer only electrons that come from external NDH [39]. In fact, the presence of both enzymes, whether associated or not, causes competition for the entrance of electrons into the respiratory chain [94].

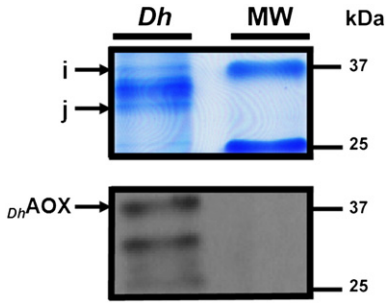

Fig. 9. Identification of the *D. hansenii* alternative oxidase (AOX) by SDS-Tricine-PAGE, western blotting and LC-MS. Total mitochondrial protein extract was subjected to SDS-Tricine-PAGE. SDS-Tricine-gel was stained with Coomassie® brilliant blue G-250 (upper panel). The SDS-Tricine-gel was electrotransferred onto PVDF membrane for western blotting. The membrane was decorated with a monoclonal mouse antibody against the AOX from the higher plant *S. guttatum* (lower panel). The two bands that were resulted immunoreactive in panel A (labeled as "i" and "j") were excised and subjected to identification by LC-MS. These results are shown in Table 5. At the upper panel, *D. hansenii* AOX corresponds to the "i" band. $_{Dh}$AOX: *Debaryomyces hansenii* alternative oxidase.

In *Y. lipolytica* growing in the exponential phase, electrons entering the respiratory chain at NDH2e are channeled to the cytochromic pathway [87]. This reflects the presence of an NDH2e-III_2-IV supercomplex. By contrast, electrons coming from pyruvate-malate (Complex I) or succinate (Complex II) can reach either the cytochromic or the alternative pathways both in *Y. lipolytica* and in *D. hansenii*. The presence of unattached non proton-pumping alternative oxidoreductases (NDH2e, $_{Mit}$GPDH, and $_{Dh}$AOX) probably constitutes a physiological mitochondrial uncoupling mechanism [35]. This is interesting, as *Y. lipolytica* seems to lack the ability to undergo a permeability transition [51,95] while *D. hansenii* does possess a mitochondrial unspecific channel [14]. Electron transfer from the alternative oxidoreductases to AOX constitutes a futile oxygen consumption pathway that needs to be tightly regulated [89]. The presence of this pathway in *D. hansenii* during the exponential growth phase is puzzling, although it may be suggested that it participates in the modulation of ROS production as has been proposed in other branched respiratory chains [35].

In *D. hansenii*, the mammalian-like mitochondrial respiratory complexes I, III and IV are associated in supercomplexes. Supramolecular organization of the respiratory chain has been proposed to promote electron channeling, stabilization of labile multi-subunit complexes and sequestration of free radicals [48]. Consistent association patterns of supercomplexes observed by BN-PAGE, strongly suggest the existence of larger structures such as "respiratory strings" [86] or "respiratory patches" [54]. In *Y. lipolytica* supercomplexes I–III_2, I-III_2-IV_4, I-IV, III_2-IV and III_2-IV_2 and a complex V dimer have been described [51]. In *S. cerevisiae* mitochondria a supercomplex III_2-IV_2 has been detected [96]. In *D. hansenii* respiratory supercomplexes involving complexes I, III and IV were similar to those found in *Y. lipolytica*. Supercomplexes I-III_2, I-III_2-IV_3 and III_2-IV_4 from *D. hansenii* contained the higher NADH dehydrogenase and COX activities as measured in BN-gels (Fig. 4C and D, lanes Dig). These supercomplexes were better observed in the activity staining experiments. In addition, the complex V dimer was easily observed both in the BN-gel and by ATPase activity staining (Fig. 4B and E, lane Dig). The *D. hansenii* F_1F_0-ATP synthase dimer was heavier than the V_2 from *Y. lipolytica*. This is probably due to stronger interactions between the subunits of complex V in these mitochondria than in other yeasts. Another explanation to this observation could be that V_2 may be associated to, and stabilized by the ATP/ADP carrier (ANC) and the phosphate carrier (PiC) in a structure known as the "synthasome" [97]. Molecular weights from the other respiratory complexes were similar to those from *Y. lipolytica*. Moreover, a big difference was observed between the single classical complexes from both *D. hansenii* and *Y. lipolytica* (Fig. 4A and B, lanes LM). In *D. hansenii* respiratory complexes were observed in smaller concentration than complex V. In fact, complex III was not observed in the BN-gels; it was only located by its subunit pattern in the 2D-SDS-Tricine-gels (Fig. 5) and by the identification of the core proteins 1 and 2 by mass

spectrometry (Table 3). Cytochromic complexes III and IV are postulated to be the scaffold of the "respiratory string" [86]. In this case, our observation is unclear, as complex III does not seem to be present in the same amount as complex IV (Fig. 4B, lane LM). These results are not clearly understood and need to be explored further. Still, the electrophoretic migration of respiratory supercomplexes, their putative MWs, their enzymatic activities and the LC-MS identification of some of their subunits indicate that the mitochondrial respiratory chain from *D. hansenii* associates into supercomplexes which are very similar to those detected in organisms studied before such as mammals [44,48,68], plants [43,45,46,50] and other yeasts such as *S. cerevisiae* [44,53] and *Y. lipolytica* [51].

This is the first description of the complete structure of the branched respiratory chain from *D. hansenii*. In addition, we analyzed the supramolecular organization of the classical respiratory complexes in *D. hansenii* mitochondria. Alternative redox enzymes from this yeast do not seem to be attached to supercomplexes at least under our experimental conditions (mid-exponential phase, non-fermentable carbon source), which suggests that the *D. hansenii* alternative oxidoreductases dynamically associate/dissociate with supercomplexes. This would be in agreement with a dynamic *plasticity* model of the oxidative phosphorylation [55], i.e. respiratory components alternate between association in supercomplexes and free forms.

Acknowledgements

Technical assistance was received from Martha Calahorra, Ramón Méndez-Franco and Norma Sánchez. We thank Dr Juan Pablo Pardo for the gift of the AOX antibody. Partially funded by the PAPIIT program and DGAPA/UNAM (grant IN202612). ACO, SGC and MRL are CONACYT fellows enrolled in the Biochemistry Graduate Program at UNAM. This is a partial requirement for the obtention of the PhD degree by ACO.

References

[1] J.C. Gonzalez-Hernandez, C.A. Cardenas-Monroy, A. Pena, Sodium and potassium transport in the halophilic yeast *Debaryomyces hansenii*, Yeast 21 (2004) 403–412.
[2] U. Breuer, H. Harms, *Debaryomyces hansenii*—an extremophilic yeast with biotechnological potential, Yeast 23 (2006) 415–437.
[3] B. Norkrans, Studies on marine occurring yeasts: growth related to pH, NaCl concentration and temperature, Arch. Mikrobiol. 54 (1966) 374–392.
[4] B. Norkrans, A. Kylin, Regulation of the potassium to sodium ratio and of the osmotic potential in relation to salt tolerance in yeasts, J. Bacteriol. 100 (1969) 836–845.
[5] C. Prista, M.C. Loureiro-Dias, V. Montiel, R. Garcia, J. Ramos, Mechanisms underlying the halotolerant way of *Debaryomyces hansenii*, FEMS Yeast Res. 5 (2005) 693–701.
[6] J.A. Hobot, D.H. Jennings, Growth of *Debaryomyces hansenii* and *Saccharomyces cerevisiae* in relation to pH and salinity, Exp. Mycol. 5 (1981) 217–228.
[7] H. Seiler, M. Busse, The yeasts of cheese brines, Int. J. Food Microbiol. 11 (1990) 289–303.
[8] T. Nakase, M. Suzuki, Taxonomic studies on *Debaryomyces hansenii* (Zopf) Lodder et Kreger-Van Rij and related species. II. Practical discrimination and nomenclature, J. Gen. Appl. Microbiol. 31 (1985) 71–86.
[9] T.v.d. Tempel, M. Jakobsen, The technological characteristics of *Debaryomyces hansenii* and *Yarrowia lipolytica* and their potential as starter cultures for production of Danablu, Int. Dairy J. 10 (2000) 263–270.
[10] M.E. Fadda, V. Mossa, M.B. Pisano, M. Deplano, S. Cosentino, Occurrence and characterization of yeasts isolated from artisanal Fiore Sardo cheese, Int. J. Food Microbiol. 95 (2004) 51–59.
[11] N.S. Sanchez, M. Calahorra, J.C. Gonzalez-Hernandez, A. Pena, Glycolytic sequence and respiration of *Debaryomyces hansenii* as compared to *Saccharomyces cerevisiae*, Yeast 23 (2006) 361–374.
[12] N.S. Sanchez, R. Arreguin, M. Calahorra, A. Pena, Effects of salts on aerobic metabolism of *Debaryomyces hansenii*, FEMS Yeast Res. 8 (2008) 1303–1312.
[13] M. Calahorra, N.S. Sanchez, A. Pena, Activation of fermentation by salts in *Debaryomyces hansenii*, FEMS Yeast Res. 9 (2009) 1293–1301.
[14] A. Cabrera-Orefice, S. Guerrero-Castillo, L.A. Luevano-Martinez, A. Pena, S. Uribe-Carvajal, Mitochondria from the salt-tolerant yeast *Debaryomyces hansenii* (halophilic organelles?), J. Bioenerg. Biomembr. 42 (2010) 11–19.
[15] M. Gutierrez-Aguilar, X. Perez-Martinez, E. Chavez, S. Uribe-Carvajal, In *Saccharomyces cerevisiae*, the phosphate carrier is a component of the mitochondrial unselective channel, Arch. Biochem. Biophys. 494 (2010) 184–191.
[16] B. Guerin, O. Bunoust, V. Rouqueys, M. Rigoulet, ATP-induced unspecific channel in yeast mitochondria, J. Biol. Chem. 269 (1994) 25406–25410.
[17] S. Manon, M. Guerin, Investigation of the yeast mitochondrial unselective channel in intact and permeabilized spheroplasts, Biochem. Mol. Biol. Int. 44 (1998) 565–575.
[18] V. Perez-Vazquez, A. Saavedra-Molina, S. Uribe, In *Saccharomyces cerevisiae*, cations control the fate of the energy derived from oxidative metabolism through the opening and closing of the yeast mitochondrial unselective channel, J. Bioenerg. Biomembr. 35 (2003) 231–241.
[19] M. Gutierrez-Aguilar, V. Perez-Vazquez, O. Bunoust, S. Manon, M. Rigoulet, S. Uribe, In yeast, Ca^{2+} and octylguanidine interact with porin (VDAC) preventing the mitochondrial permeability transition, Biochim. Biophys. Acta 1767 (2007) 1245–1251.
[20] D.G. Nicholls, S.J. Ferguson, Bioenergetics 3, Academic Press, London, 2002.
[21] T. Joseph-Horne, D.W. Hollomon, P.M. Wood, Fungal respiration: a fusion of standard and alternative components, Biochim. Biophys. Acta 1504 (2001) 179–195.
[22] I.M. Juszczuk, A.M. Rychter, Alternative oxidase in higher plants, Acta Biochim. Pol. 50 (2003) 1257–1271.
[23] N. Sen, H.K. Majumder, Mitochondrion of protozoan parasite emerges as potent therapeutic target: exciting drugs are on the horizon, Curr. Pharm. Des. 14 (2008) 839–846.
[24] A. McDonald, G. Vanlerberghe, Branched mitochondrial electron transport in the Animalia: presence of alternative oxidase in several animal phyla, IUBMB Life 56 (2004) 333–341.
[25] D. Munro, N. Pichaud, F. Paquin, V. Kemeid, P.U. Blier, Low hydrogen peroxide production in mitochondria of the long-lived *Arctica islandica*: underlying mechanisms for slow aging, Aging cell 12 (2013) 584–592.
[26] R. Buschges, G. Bahrenberg, M. Zimmermann, K. Wolf, NADH: ubiquinone oxidoreductase in obligate aerobic yeasts, Yeast 10 (1994) 475–479.
[27] J. Nosek, H. Fukuhara, NADH dehydrogenase subunit genes in the mitochondrial DNA of yeasts, J. Bacteriol. 176 (1994) 5622–5630.
[28] D.A. Berthold, M.E. Andersson, P. Nordlund, New insight into the structure and function of the alternative oxidase, Biochim. Biophys. Acta 1460 (2000) 241–254.
[29] M.S. Albury, C. Affourtit, P.G. Crichton, A.L. Moore, Structure of the plant alternative oxidase. Site-directed mutagenesis provides new information on the active site and membrane topology, J. Biol. Chem. 277 (2002) 1190–1194.
[30] M.E. Andersson, P. Nordlund, A revised model of the active site of alternative oxidase, FEBS Lett. 449 (1999) 17–22.
[31] A.L. Moore, J.N. Siedow, The regulation and nature of the cyanide-resistant alternative oxidase of plant mitochondria, Biochim. Biophys. Acta 1059 (1991) 121–140.
[32] H. Lambers, The physiological significance of the cyanide-resistant respiration in higher plants, Plant Cell Environ. 3 (1980) 293–302.
[33] D.A. Day, J.T. Wiskich, Regulation of alternative oxidase activity in higher plants, J. Bioenerg. Biomembr. 27 (1995) 379–385.
[34] D.P. Maxwell, Y. Wang, L. McIntosh, The alternative oxidase lowers mitochondrial reactive oxygen production in plant cells, Proc. Natl. Acad. Sci. U. S. A. 96 (1999) 8271–8276.
[35] S. Guerrero-Castillo, D. Araiza-Olivera, A. Cabrera-Orefice, J. Espinasa-Jaramillo, M. Gutierrez-Aguilar, L.A. Luevano-Martinez, A. Zepeda-Bastida, S. Uribe-Carvajal, Physiological uncoupling of mitochondrial oxidative phosphorylation. Studies in different yeast species, J. Bioenerg. Biomembr. 43 (2011) 323–331.
[36] R. El-Khoury, E. Dufour, M. Rak, N. Ramanantsoa, N. Grandchamp, Z. Csaba, B. Duvillie, P. Benit, J. Gallego, P. Gressens, C. Sarkis, H.T. Jacobs, P. Rustin, Alternative oxidase expression in the mouse enables bypassing cytochrome c oxidase blockade and limits mitochondrial ROS overproduction, PLoS Genet. 9 (2013) e1003182.
[37] S. Kerscher, S. Drose, V. Zickermann, U. Brandt, The three families of respiratory NADH dehydrogenases, Results Probl. Cell Differ. 45 (2008) 185–222.
[38] S. de Vries, L.A. Grivell, Purification and characterization of a rotenone-insensitive NADH:Q6 oxidoreductase from mitochondria of *Saccharomyces cerevisiae*, Eur. J. Biochem. 176 (1988) 377–384.
[39] I.L. Pahlman, C. Larsson, N. Averet, O. Bunoust, S. Boubekeur, L. Gustafsson, M. Rigoulet, Kinetic regulation of the mitochondrial glycerol-3-phosphate dehydrogenase by the external NADH dehydrogenase in *Saccharomyces cerevisiae*, J. Biol. Chem. 277 (2002) 27991–27995.
[40] M. Rigoulet, A. Mourier, A. Galinier, L. Casteilla, A. Devin, Electron competition process in respiratory chain: regulatory mechanisms and physiological functions, Biochim. Biophys. Acta 1797 (2010) 671–677.
[41] B. Ronnow, M.C. Kielland-Brandt, GUT2, a gene for mitochondrial glycerol 3-phosphate dehydrogenase of *Saccharomyces cerevisiae*, Yeast 9 (1993) 1121–1130.
[42] C.R. Hackenbrock, B. Chazotte, S.S. Gupte, The random collision model and a critical assessment of diffusion and collision in mitochondrial electron transport, J. Bioenerg. Biomembr. 18 (1986) 331–368.
[43] H. Eubel, J. Heinemeyer, H.P. Braun, Identification and characterization of respirasomes in potato mitochondria, Plant Physiol. 134 (2004) 1450–1459.
[44] H. Schagger, K. Pfeiffer, Supercomplexes in the respiratory chains of yeast and mammalian mitochondria, EMBO J. 19 (2000) 1777–1783.
[45] F. Krause, N.H. Reifschneider, D. Vocke, H. Seelert, S. Rexroth, N.A. Dencher, "Respirasome"-like supercomplexes in green leaf mitochondria of spinach, J. Biol. Chem. 279 (2004) 48369–48375.
[46] H. Eubel, L. Jansch, H.P. Braun, New insights into the respiratory chain of plant mitochondria. Supercomplexes and a unique composition of complex II, Plant Physiol. 133 (2003) 274–286.
[47] G. Lenaz, M.L. Genova, Kinetics of integrated electron transfer in the mitochondrial respiratory chain: random collisions vs. solid state electron channeling, Am. J. Physiol. Cell Physiol. 292 (2007) C1221–C1239.
[48] H. Schagger, Respiratory chain supercomplexes of mitochondria and bacteria, Biochim. Biophys. Acta 1555 (2002) 154–159.
[49] H. Schagger, Respiratory chain supercomplexes, IUBMB Life 52 (2001) 119–128.
[50] N.V. Dudkina, J. Heinemeyer, S. Sunderhaus, E.J. Boekema, H.P. Braun, Respiratory chain supercomplexes in the plant mitochondrial membrane, Trends Plant Sci. 11 (2006) 232–240.

[51] S. Guerrero-Castillo, M. Vazquez-Acevedo, D. Gonzalez-Halphen, S. Uribe-Carvajal, In *Yarrowia lipolytica* mitochondria, the alternative NADH dehydrogenase interacts specifically with the cytochrome complexes of the classic respiratory pathway, Biochim. Biophys. Acta 1787 (2009) 75–85.
[52] H. Boumans, L.A. Grivell, J.A. Berden, The respiratory chain in yeast behaves as a single functional unit, J. Biol. Chem. 273 (1998) 4872–4877.
[53] R.A. Stuart, Supercomplex organization of the oxidative phosphorylation enzymes in yeast mitochondria, J. Bioenerg. Biomembr. 40 (2008) 411–417.
[54] E. Nubel, I. Wittig, S. Kerscher, U. Brandt, H. Schagger, Two-dimensional native electrophoretic analysis of respiratory supercomplexes from *Yarrowia lipolytica*, Proteomics 9 (2009) 2408–2418.
[55] R. Acin-Perez, P. Fernandez-Silva, M.L. Peleato, A. Perez-Martos, J.A. Enriquez, Respiratory active mitochondrial supercomplexes, Mol. Cell 32 (2008) 529–539.
[56] E.J. Boekema, H.P. Braun, Supramolecular structure of the mitochondrial oxidative phosphorylation system, J. Biol. Chem. 282 (2007) 1–4.
[57] A. Veiga, J.D. Arrabaca, M.C. Loureiro-Dias, Cyanide-resistant respiration is frequent, but confined to yeasts incapable of aerobic fermentation, FEMS Microbiol. Lett. 190 (2000) 93–97.
[58] A. Veiga, J.D. Arrabaca, M.C. Loureiro-Dias, Cyanide-resistant respiration, a very frequent metabolic pathway in yeasts, FEMS Yeast Res. 3 (2003) 239–245.
[59] A. Veiga, J.D. Arrabaca, F. Sansonetty, P. Ludovico, M. Corte-Real, M.C. Loureiro-Dias, Energy conversion coupled to cyanide-resistant respiration in the yeasts *Pichia membranifaciens* and *Debaryomyces hansenii*, FEMS Yeast Res. 3 (2003) 141–148.
[60] A.G. Gornall, C.J. Bardawill, M.M. David, Determination of serum proteins by means of the biuret reaction, J. Biol. Chem. 177 (1949) 751–766.
[61] I. Wittig, H. Schagger, Advantages and limitations of clear-native PAGE, Proteomics 5 (2005) 4338–4346.
[62] B.R. Oakley, D.R. Kirsch, N.R. Morris, A simplified ultrasensitive silver stain for detecting proteins in polyacrylamide gels, Anal. Biochem. 105 (1980) 361–363.
[63] W. Wray, T. Boulikas, V.P. Wray, R. Hancock, Silver staining of proteins in polyacrylamide gels, Anal. Biochem. 118 (1981) 197–203.
[64] E. Zerbetto, L. Vergani, F. Dabbeni-Sala, Quantification of muscle mitochondrial oxidative phosphorylation enzymes via histochemical staining of blue native polyacrylamide gels, Electrophoresis 18 (1997) 2059–2064.
[65] M.S. Johnson, S.A. Kuby, Studies on NADH (NADPH)-cytochrome c reductase (FMN-containing) from yeast. Isolation and physicochemical properties of the enzyme from top-fermenting ale yeast, J. Biol. Chem. 260 (1985) 12341–12350.
[66] U. Brandt, A two-state stabilization-change mechanism for proton-pumping complex I, Biochim. Biophys. Acta 1807 (2011) 1364–1369.
[67] M. Iwata, Y. Lee, T. Yamashita, T. Yagi, S. Iwata, A.D. Cameron, M.J. Maher, The structure of the yeast NADH dehydrogenase (Ndi1) reveals overlapping binding sites for water- and lipid-soluble substrates, Proc. Natl. Acad. Sci. U. S. A. 109 (2012) 15247–15252.
[68] I. Wittig, M. Karas, H. Schagger, High resolution clear native electrophoresis for in-gel functional assays and fluorescence studies of membrane protein complexes, Mol. Cell. Proteomics 6 (2007) 1215–1225.
[69] B. Dujon, D. Sherman, G. Fischer, P. Durrens, S. Casaregola, I. Lafontaine, J. De Montigny, C. Marck, C. Neuveglise, E. Talla, N. Goffard, L. Frangeul, M. Aigle, V. Anthouard, A. Babour, V. Barbe, S. Barnay, S. Blanchin, J.M. Beckerich, E. Beyne, C. Bleykasten, A. Boisrame, J. Boyer, L. Cattolico, F. Confanioleri, A. De Daruvar, L. Despons, E. Fabre, C. Fairhead, H. Ferry-Dumazet, A. Groppi, F. Hantraye, C. Hennequin, N. Jauniaux, P. Joyet, R. Kachouri, A. Kerrest, R. Koszul, M. Lemaire, I. Lesur, L. Ma, H. Muller, J.M. Nicaud, M. Nikolski, S. Oztas, O. Ozier-Kalogeropoulos, S. Pellenz, S. Potier, G.F. Richard, M.L. Straub, A. Suleau, D. Swennen, F. Tekaia, M. Wesolowski-Louvel, E. Westhof, B. Wirth, M. Zeniou-Meyer, I. Zivanovic, M. Bolotin-Fukuhara, A. Thierry, C. Bouchier, B. Caudron, C. Scarpelli, C. Gaillardin, J. Weissenbach, P. Wincker, J.L. Souciet, Genome evolution in yeasts, Nature 430 (2004) 35–44.
[70] D.J. Sherman, T. Martin, M. Nikolski, C. Cayla, J.L. Souciet, P. Durrens, Genolevures: protein families and synteny among complete hemiascomycetous yeast proteomes and genomes, Nucleic Acids Res. 37 (2009) D550–D554.
[71] W.K. Huh, S.O. Kang, Characterization of the gene family encoding alternative oxidase from *Candida albicans*, Biochem. J. 356 (2001) 595–604.
[72] M.A. Larkin, G. Blackshields, N.P. Brown, R. Chenna, P.A. McGettigan, H. McWilliam, F. Valentin, I.M. Wallace, A. Wilm, R. Lopez, J.D. Thompson, T.J. Gibson, D.G. Higgins, Clustal W and Clustal X version 2.0, Bioinformatics 23 (2007) 2947–2948.
[73] U.K. Laemmli, Cleavage of structural proteins during the assembly of the head of bacteriophage T4, Nature 227 (1970) 680–685.
[74] H. Towbin, T. Staehelin, J. Gordon, Electrophoretic transfer of proteins from polyacrylamide gels to nitrocellulose sheets: procedure and some applications, Proc. Natl. Acad. Sci. U. S. A. 76 (1979) 4350–4354.
[75] T.E. Elthon, R.L. Nickels, L. McIntosh, Monoclonal antibodies to the alternative oxidase of higher plant mitochondria, Plant Physiol. 89 (1989) 1311–1317.
[76] N. Chiquete-Felix, J.M. Hernandez, J.A. Mendez, A. Zepeda-Bastida, A. Chagolla-Lopez, A. Mujica, In guinea pig sperm, aldolase A forms a complex with actin, WAS, and Arp2/3 that plays a role in actin polymerization, Reproduction 137 (2009) 669–678.
[77] S.J. Kerscher, J.G. Okun, U. Brandt, A single external enzyme confers alternative NADH:ubiquinone oxidoreductase activity in *Yarrowia lipolytica*, J. Cell Sci. 112 (Pt 14) (1999) 2347–2354.
[78] M.G. Claros, P. Vincens, Computational method to predict mitochondrially imported proteins and their targeting sequences, Eur. J. Biochem. 241 (1996) 779–786.
[79] L. Adler, A. Blomberg, A. Nilsson, Glycerol metabolism and osmoregulation in the salt-tolerant yeast *Debaryomyces hansenii*, J. Bacteriol. 162 (1985) 300–306.
[80] A.L. Umbach, J.N. Siedow, The cyanide-resistant alternative oxidases from the fungi *Pichia stipitis* and *Neurospora crassa* are monomeric and lack regulatory features of the plant enzyme, Arch. Biochem. Biophys. 378 (2000) 234–245.
[81] C. Affourtit, K. Krab, A.L. Moore, Control of plant mitochondrial respiration, Biochim. Biophys. Acta 1504 (2001) 58–69.
[82] C.A. Smith, V.J. Melino, C. Sweetman, K.L. Soole, Manipulation of alternative oxidase can influence salt tolerance in *Arabidopsis thaliana*, Physiol. Plant. 137 (2009) 459–472.
[83] S. Sakajo, N. Minagawa, T. Komiyama, A. Yoshimoto, Characterization of cyanide-resistant respiration and appearance of a 36 kDa protein in mitochondria isolated from antimycin A-treated *Hansenula anomala*, J. Biochem. 108 (1990) 166–168.
[84] X. Huang, U. von Rad, J. Durner, Nitric oxide induces transcriptional activation of the nitric oxide-tolerant alternative oxidase in *Arabidopsis* suspension cells, Planta 215 (2002) 914–923.
[85] O. Juarez, G. Guerra, F. Martinez, J.P. Pardo, The mitochondrial respiratory chain of *Ustilago maydis*, Biochim. Biophys. Acta 1658 (2004) 244–251.
[86] I. Wittig, R. Carrozzo, F.M. Santorelli, H. Schagger, Supercomplexes and subcomplexes of mitochondrial oxidative phosphorylation, Biochim. Biophys. Acta 1757 (2006) 1066–1072.
[87] S. Guerrero-Castillo, A. Cabrera-Orefice, M. Vazquez-Acevedo, D. Gonzalez-Halphen, S. Uribe-Carvajal, During the stationary growth phase, *Yarrowia lipolytica* prevents the overproduction of reactive oxygen species by activating an uncoupled mitochondrial respiratory pathway, Biochim. Biophys. Acta 1817 (2012) 353–362.
[88] X. Grandier-Vazeille, K. Bathany, S. Chaignepain, N. Camougrand, S. Manon, J.M. Schmitter, Yeast mitochondrial dehydrogenases are associated in a supramolecular complex, Biochemistry 40 (2001) 9758–9769.
[89] S. Uribe-Carvajal, L.A. Luevano-Martinez, S. Guerrero-Castillo, A. Cabrera-Orefice, N.A. Corona-de-la-Pena, M. Gutierrez-Aguilar, Mitochondrial unselective channels throughout the eukaryotic domain, Mitochondrion 11 (2011) 382–390.
[90] S.J. Kerscher, Diversity and origin of alternative NADH:ubiquinone oxidoreductases, Biochim. Biophys. Acta 1459 (2000) 274–283.
[91] S.A. Uyemura, S. Luo, M. Vieira, S.N. Moreno, R. Docampo, Oxidative phosphorylation and rotenone-insensitive malate- and NADH-quinone oxidoreductases in *Plasmodium yoelii yoelii* mitochondria in situ, J. Biol. Chem. 279 (2004) 385–393.
[92] V.P. Martins, F.M. Soriani, T. Magnani, V.G. Tudella, G.H. Goldman, C. Curti, S.A. Uyemura, Mitochondrial function in the yeast form of the pathogenic fungus *Paracoccidioides brasiliensis*, J. Bioenerg. Biomembr. 40 (2008) 297–305.
[93] M. Klingenberg, Localization of the glycerol-phosphate dehydrogenase in the outer phase of the mitochondrial inner membrane, Eur. J. Biochem. 13 (1970) 247–252.
[94] O. Bunoust, A. Devin, N. Averet, N. Camougrand, M. Rigoulet, Competition of electrons to enter the respiratory chain: a new regulatory mechanism of oxidative metabolism in *Saccharomyces cerevisiae*, J. Biol. Chem. 280 (2005) 3407–3413.
[95] M.V. Kovaleva, E.I. Sukhanova, T.A. Trendeleva, M.V. Zyl'kova, L.A. Ural'skaya, K.M. Popova, N.E. Saris, R.A. Zvyagilskaya, Induction of a non-specific permeability transition in mitochondria from *Yarrowia lipolytica* and *Dipodascus* (*Endomyces*) *magnusii* yeasts, J. Bioenerg. Biomembr. 41 (2009) 239–249.
[96] J. Heinemeyer, H.P. Braun, E.J. Boekema, R. Kouril, A structural model of the cytochrome C reductase/oxidase supercomplex from yeast mitochondria, J. Biol. Chem. 282 (2007) 12240–12248.
[97] C. Chen, Y. Ko, M. Delannoy, S.J. Ludtke, W. Chiu, P.L. Pedersen, Mitochondrial ATP synthasome: three-dimensional structure by electron microscopy of the ATP synthase in complex formation with carriers for Pi and ADP/ATP, J. Biol. Chem. 279 (2004) 31761–31768.